

Update on developments at SNIF

J. Zacks, I. Turner, I. Day, K. Flinders, B. Crowley, and R. McAdams

Citation: *AIP Conference Proceedings* **1655**, 030012 (2015);

View online: <https://doi.org/10.1063/1.4916439>

View Table of Contents: <http://aip.scitation.org/toc/apc/1655/1>

Published by the *American Institute of Physics*

Update on Developments at SNIF

J. Zacks^{1, a)}, I. Turner¹, I. Day¹, K. Flinders¹, B. Crowley², R. McAdams¹

¹CCFE, Culham Science Centre, Abingdon, Oxfordshire, OX14 3TR, UK

²General Atomics, PO Box 85608, San Diego, California 92186-5608, USA

^{a)}Corresponding author: jamie.zacks@ccfe.ac.uk

Abstract. The Small Negative Ion Facility (SNIF) at CCFE has been undergoing continuous development and enhancement to both improve operational reliability and increase diagnostic capability. SNIF uses a CW 13.56MHz, 5kW RF driven volume source with a 30kV triode accelerator. Improvement and characterisation work includes:

- Installation of a new “L” type RF matching unit, used to calculate the load on the RF generator.
- Use of the electron suppressing biased insert as a Langmuir probe under different beam extraction conditions.
- Measurement of the hydrogen Fulcher molecular spectrum, used to calculate gas temperature in the source.
- Beam optimisation through parameter scans, using copper target plate and visible cameras, with results compared with AXCEL-INP to provide beam current estimate.
- Modelling of the beam power density profile on the target plate using ANSYS to estimate beam power and provide another estimate of beam current.

This work is described, and has allowed an estimation of the extracted beam current of approximately 6mA (4mA/cm²) at 3.5kW RF power and a source pressure of 0.6Pa.

INTRODUCTION

The Small Negative Ion Facility (SNIF) at CCFE [1] has been undergoing continuing development. A new “L” type matching unit has been installed to replace the “Pi” type unit previously used. This new unit is better designed to withstand the load of the SNIF ion source (Fig. 1), allowing full exploitation of the 5kW, 13.56MHz power supply. Along with the installation of a water polishing column, this has allowed improved beam extraction using the 30kV triode accelerator. Characterisation measurements of the RF loads are presented with the new matching unit, as well as a measurement of the hysteresis of the transition between capacitive and inductive coupling modes.

To further aid in source characterisation, a Baratron pressure gauge was connected to the source to measure the source filling pressure with different gas flow rates. It was found that the regularly used flow rate of 10sccm gave a source filling pressure of 0.59Pa.

The above operational improvements have allowed development to progress on the SNIF diagnostic systems. The instrumented beam target has been used to collect data on the beam profile, allowing optimisation of the beam through variation of the output from the 6kV extraction power supply. Due to the small extraction area (radius=0.7cm, area = 1.54cm²), beam pulse lengths greater than 20s are necessary for temperature rises to be seen, and have shown that a 1D heat transfer model is inadequate for deriving the power density profile. Instead, thermal modelling using the ANSYS software has been performed, with the initial results presented.

Further analysis of the beam profile was performed using visible cameras mounted on the side of the beamline vacuum tank. This confirmed the extraction voltage optimisation, though highlighted a feature of the beam profile which is still to be fully investigated.

The biased (w.r.t the plasma grid voltage) insert used for suppression of co-extracted electrons was used as a Langmuir probe, to measure changes in the properties of the extraction region with varying extraction voltage. Estimates of electron temperature were then combined with spectrometer measurements of the Fulcher molecular band to obtain an estimate of the gas temperature achieved in the source.

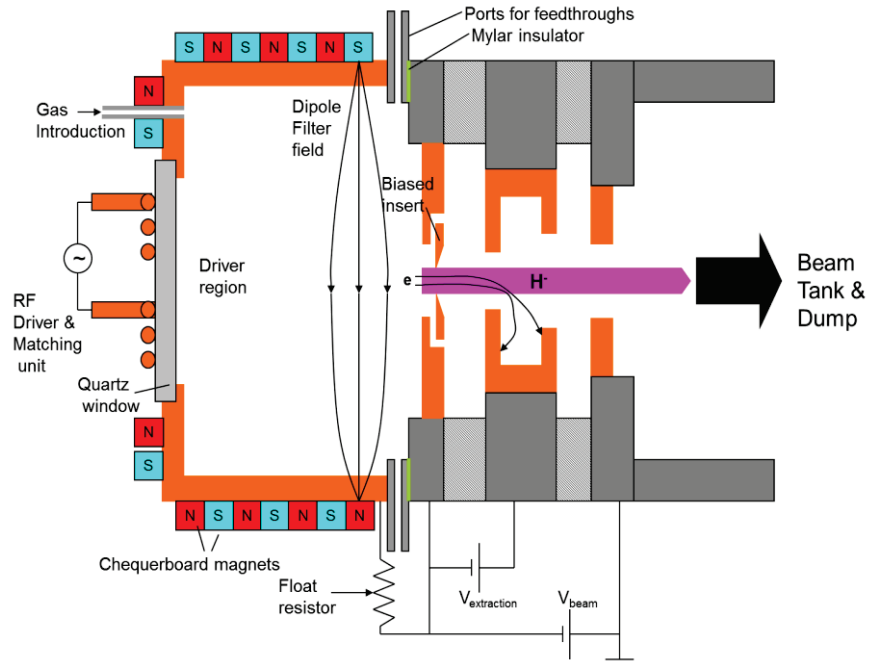


FIGURE 1. The SNIF RF Driven Source and electron suppressing accelerator

SOURCE DEVELOPMENT AND CHARACTERISATION

Matching Unit Upgrade

The original RF matching unit on SNIF was not able to withstand the source load at powers above 1.5kW, where voltages $\sim 6\text{kV}$ and currents $\sim 100\text{A}$ were generated within the circuit [1]. Therefore a water-cooled Seren ATS Series matching unit was purchased, with specifications designed to reduce these voltages and currents to a level ($\sim 3\text{kV}, 30\text{A}$) tolerable by the matching unit. This unit contains two variable capacitors, tuneable from 250-1000pF, in an “L” configuration (see Fig. 2). The Load capacitor is seen to vary with slightly with RF power, whereas the Tune capacitor shows little response.

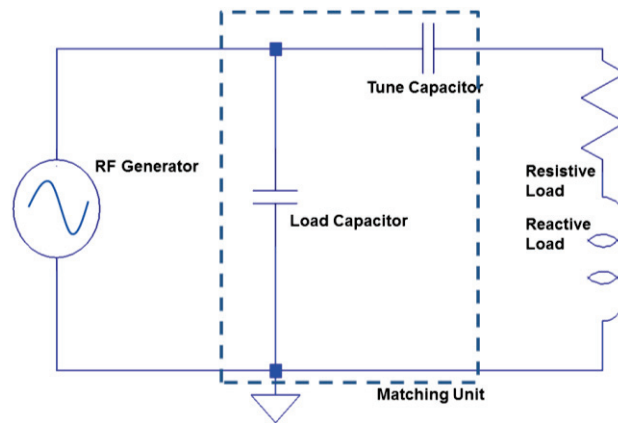


FIGURE 2. Diagram of the “L” circuit within the SNIF matching unit. Plasma load is shown as both resistive and reactive components.

Load Calculations

As performed previously [1] through solving of the circuit equations, the positions of the capacitors at full match were used to calculate the resistive and reactive loads of the antenna and source system as a function of power (see Fig. 3). Differences in the values were seen when compared to the previous measurements, however this is

considered to be the result of the significant changes made to the system between the matching unit and the source as a result of purchasing a new unit.

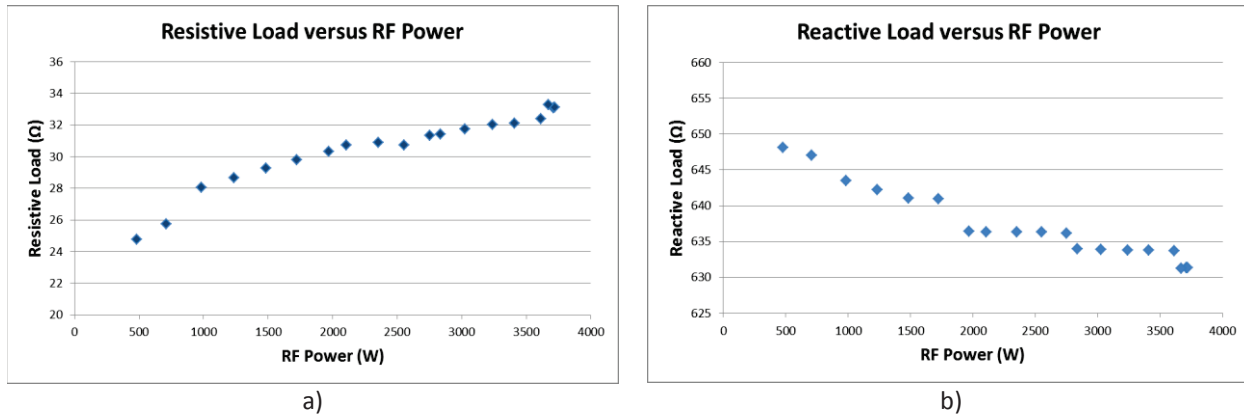


FIGURE 3. a) Resistive and b) Reactive loads for the SNIF ion source and antenna system.

E-H Transition Hysteresis

The transition between capacitive (E) and inductive (H) modes in RF driven plasmas is known to show a hysteresis in the transition region. The phenomenon has been attributed to a non-linearity in the absorbed or dissipated power at low electron density [2]. As well as the stepped increase in luminosity, the transition from E to H mode also changes the match requirements of the matching unit, and a step change is seen on the Load Capacitor. The source was operated with a slow ramp up of RF power, followed by a slow ramp down, with the Load Capacitor position shown in Fig. 4. A hysteresis width of approximately 200W can be seen in the SNIF RF system.

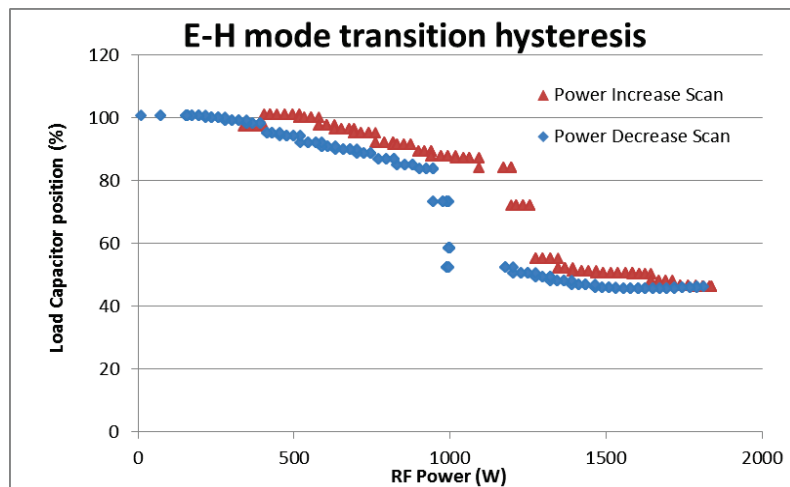


FIGURE 4. E-H transition hysteresis shown through the position of the matching Load capacitor.

Biased Insert V-I Scans

The insert plate at the extraction aperture (see Fig. 1) can be biased up to 40V and has an exposed surface area $\sim 6.5\text{cm}^2$. Variation of the voltage in the plate shows a similar response to that expected from a Langmuir probe [3], and voltage scans have been performed at a source power and gas flow of 1.2kW and 10sccm respectively, with 25kV beam voltage and a range of extraction voltages. A scan was also performed with no HV extraction. The results in Fig. 5 show some variation with extraction voltage. The reduction in electron saturation current with extraction voltage may be due to the electric field from the extraction grid penetrating further into the extraction region at higher voltage, and extracting more electrons from within the capture range of the insert. RF fields are known [4] to perturb analysis of the probe using normal Langmuir theory, through a broadening of the transition region from ion to electron saturation. However, an estimate of electron temperature T_e was still made from the low voltage part of the transition, with results given in Fig. 6. These results give a low temperature as would be

expected of the extraction region in a source with a magnetic dipole filter. Together with the positive ion saturation current, the temperature was used to obtain an estimate of plasma density $\sim 5 \times 10^{16} \text{ m}^{-3}$.

As well as suppression plate current being measured, the variation of drain current on the beam voltage power supply was measured as a function of suppression voltage. The decrease in current shown in Fig. 7 is as expected with both negative hydrogen ions and electrons being suppressed at higher voltage.

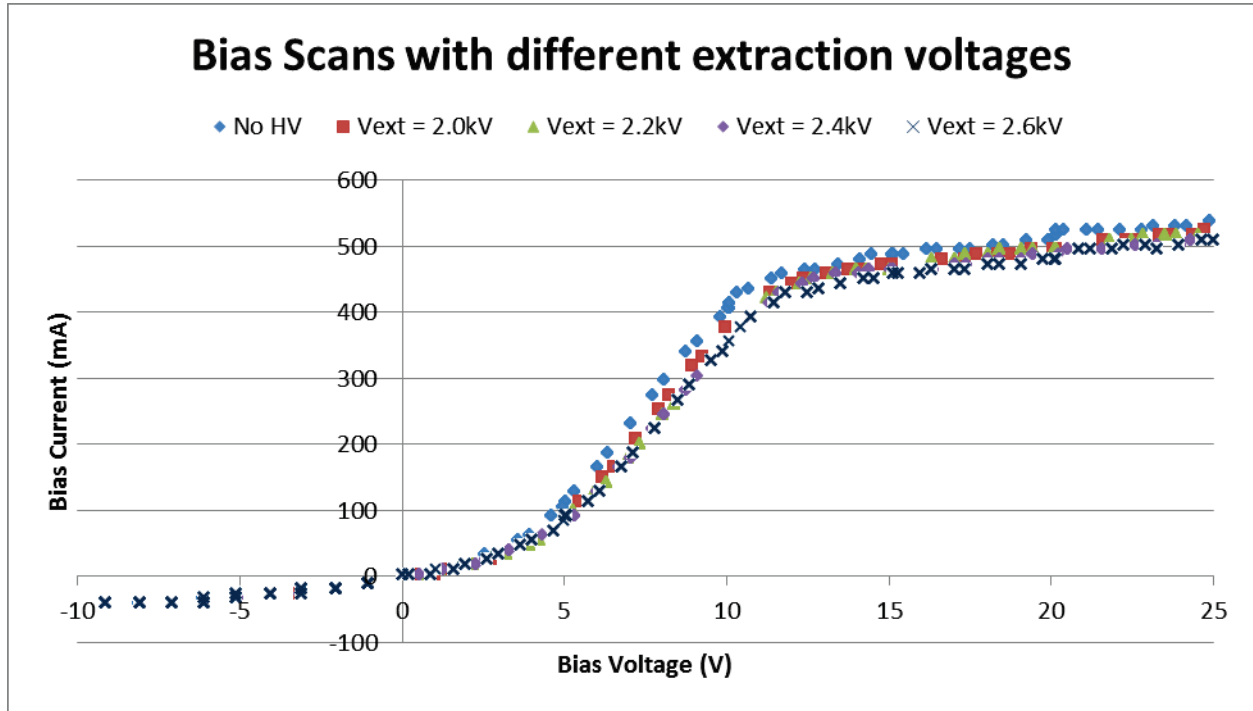


FIGURE 5. I-V traces obtained from biased insert for different extraction voltages. Other parameters are, $Q_{\text{gas}} = 10 \text{ sccm}$, $V_{\text{beam}} = 25 \text{ kV}$, $P_{\text{RF}} = 1.2 \text{ kW}$.

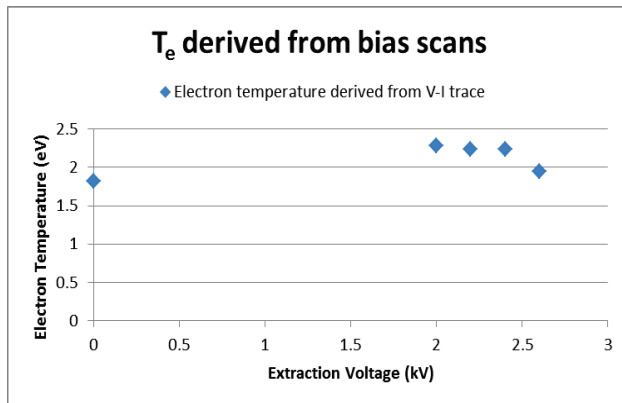


FIGURE 6. Electron temperature derived using Langmuir probe theory from data in Fig. 5.

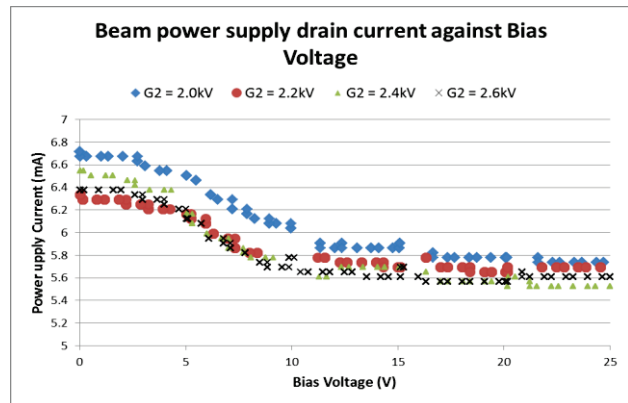


FIGURE 7. Beam power supply drain current versus biased insert voltage for different extraction voltages.

Fulcher Analysis

A McPherson 209 spectrometer with an Andor Newton CCD detector was set up with a line of sight through the extraction region of the source, using one of the feedthrough ports on the side (see Fig. 1). Measurements of the Q(0-

0) branch of the Fulcher α spectrum were made for a 3.3kW plasma, 10sccm gas flow with 4V bias, 2.6kV extraction and 25kV beam voltage, with the spectral lines shown in Fig. 8. Adopting the approach of Surrey and Crowley [5], a calculation of the translational gas temperature was made. This required measurement of the intensities of this Q branch, as well as knowledge of the electron temperature and vibrational temperature.

The electron temperature was taken as 2eV, based on the estimates made from the Bias V-I scans in the previous section. The vibrational temperature was taken to be 0.5eV. This temperature is similar in magnitude to those reported by Fantz [6], though it was found that variation of this parameter has only a small effect on the calculated gas temperature. The calculation gives a gas temperature in the region of 1400K, which is again comparable to the results in [6].

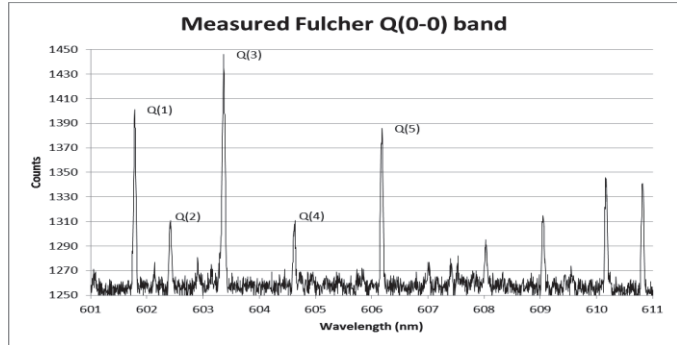


FIGURE 8. The Q(0-0) band of the hydrogen Fulcher spectrum recorded on SNIF pulse 3250.

BEAM CHARACTERISATION

Beam Optimisation and Profile Measurement

In order to improve measurements of the beam profile and power density, a series of parameter scans were performed to optimise the beam extraction for minimum divergence. The first of these scans was for the optimum extraction voltage, with the source operated at 3.5kW, 10sccm, with beam voltage of 25kV, and bias suppression of 10V.

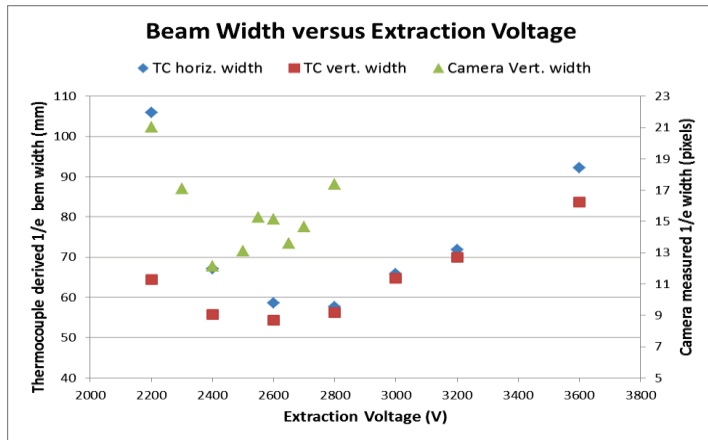


FIGURE 9. Extraction voltage scan for beam optimization, showing thermocouple (TC) and camera derived beam widths.

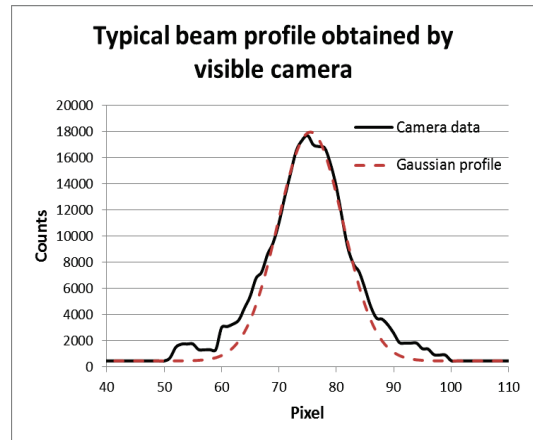


FIGURE 10. Beam profile obtained using camera view and ImageJ, compared to a typical Gaussian profile.

Figure 9 shows the variation of width as measured on the target plate. The target plate is located approximately 4m downstream of the plasma grid, and is a 12cm diameter copper plate with a grid of 4mm by 4mm castellations with 10mm deep gaps of 1mm. Over 100 thermocouples are arrayed within the castellations to provide a measurement of beam profile and power density. By fitting a 2D Gaussian to the temperature rise profile, a width was obtained to aid in beam optimisation. The vertical data was found more reliable for fitting a width to.

With the optimum extraction voltage found to be 2.6kV from the more reliable vertical width, the other parameters were scanned in turn, and small adjustments made as necessary. The V_{ext} scan was repeated with measurements taken from a visible camera located approximately 1.5m downstream of the plasma grid. The freely

available software ImageJ was used to extract the intensity profile of the beam and fit a Gaussian distribution to the intensity. The beam profile, shown in Fig. 10, can be seen to have a broad tail inconsistent with a Gaussian distribution. The cause of this is currently unknown and will be further investigated. One possible cause is deflection by the electron suppression magnets within the accelerator, and this feature may only be seen in the plane perpendicular to the bend plane of the beam. This will be verified using a second camera with a line of sight in the bend plane.

Co-extracted electrons prevent relying on the HV drain current as an accurate measure of negative ion current. Although the suppression voltage can be increased, this will also reduce the current of negative ions extracted. The power loading on the target plate can be used to calculate beam power and hence negative ion current however, as discussed in the next section, this has not proved simple. A method for estimating the beam current is to model the accelerator for the optimised beam voltages, varying the current in order to optimise the divergence within the model. This has been done using the AXCEL-INP accelerator simulation software. A plot of divergence with current density is shown in Fig. 11. It can be seen that minimum divergence occurs over a range of 40-60Am⁻².

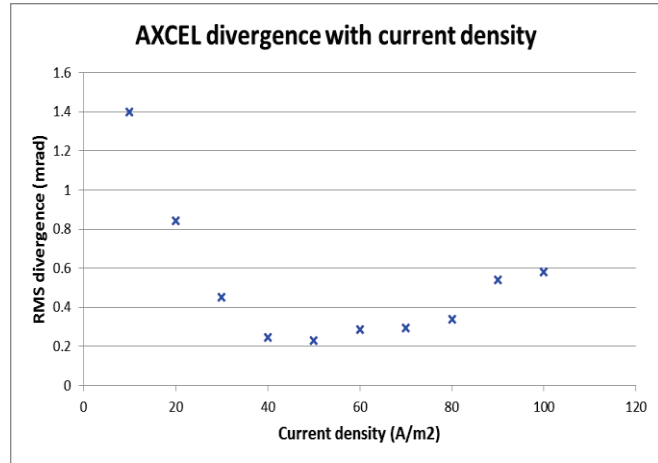


FIGURE 11. AXCEL current density scan for optimised accelerator parameters of $V_{beam} = 25kV$, $V_{ext} = 2.6kV$, $V_{bias} = 10V$.

Power Load Calculations

Due to the low power of the SNIF beam, a minimum of 15s pulse length is required to get sufficient heat rise recorded on the target plate (see Fig. 12) thermocouples for analysis. As pulse lengths up to 30s were run, it was seen that the 1D model used for power density calculations on JET [7] gave different average power densities for different pulse lengths. The likely cause of this was considered to be the much greater density of castellations allowing heat flow between castellations and perturbing the calculation on any single thermocouple. In order to provide a full heat flow model, the software ANSYS was used to try to reproduce the shape of the temperature rise seen on the target plate thermocouples. The CAD drawings of the target plate were loaded into ANSYS and through modelling the power density on different castellations, the underlying processes in the target plate heat flow were highlighted.

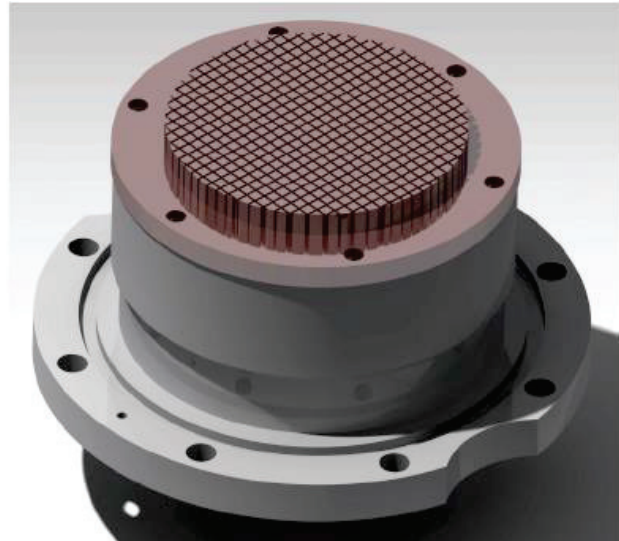


FIGURE 12. CAD rendering of the SNIF castellated copper beam target plate.

As well as the density of castellations, it was found that the beamline vacuum tank was acting as a heat sink for the target plate, and was a much larger perturbation than that caused by the high density of castellations.

Due to current limitations in the modelling code, a smooth Gaussian beam profile has not yet been implemented in ANSYS. Instead the heat load on the target plate castellations has been approximated into 7 concentric rings, each with its own uniform power density. Current modelling work has focused on adjusting the input power density

to match both the profile of temperature rises, and the shape of the rise on the central thermocouple. Figures 13 and 14 show a cross section of the input power density, with the resultant temperature rise, compared to the measured temperature rise. Figure 15 shows the time trace for the central thermocouple, with two modelled curves overlaid. The first is the one obtained from the profile used in Fig. 13, and the second used a uniform input power density found to best match the temperature rise seen on only this specific thermocouple. Modelling so far does suggest the beam profile is flatter than previously expected, though Fig. 15 shows that more work is required to obtain a good match.

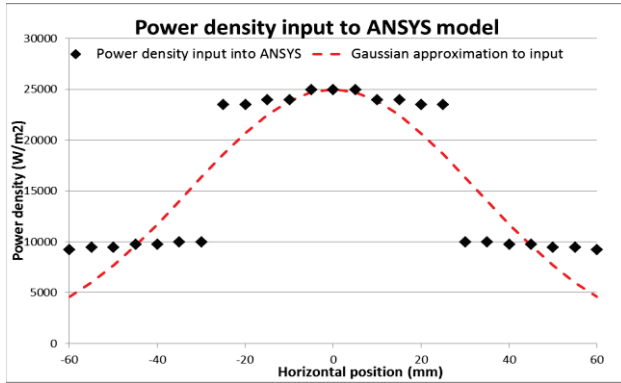


FIGURE 13. Power input profile used in ANSYS, with a Gaussian approximation shown for comparison.

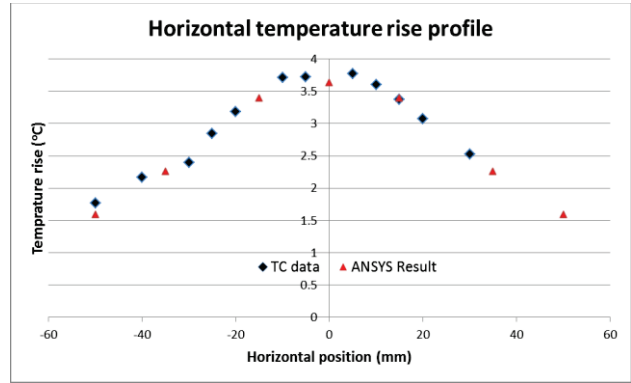


FIGURE 14. ANSYS calculated temperature rise compared with measurements from SNIF pulse 3241 (30s beam).

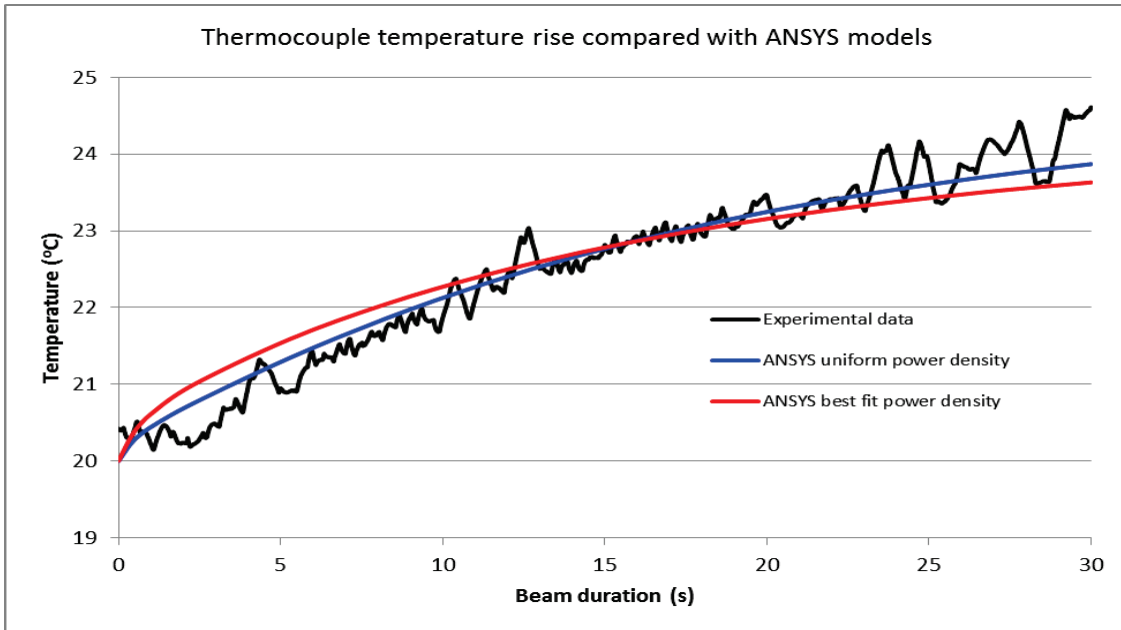


FIGURE 15. Temperature rise seen on the thermocouple at centre of beam, compared to ANSYS output for uniform power density input, and for the power input shown in Fig. 13. $P_{RF} = 3.5\text{kW}$, $Q_{\text{gas}} = 10\text{sccm}$, $V_{\text{beam}} = 25\text{kV}$, $V_{\text{ext}} = 2.6\text{kV}$.

The total power from the profile in Fig. 13 was found to be 148W. For a 25kV beam, this gives an estimated beam current of 6mA ($\sim 4\text{mAcm}^{-2}$), which is close to the current seen by the HV power supply as seen in Fig. 7, and in the region of low divergence modelled by AXCEL in Fig. 11.

SUMMARY AND FUTURE PLANS

The Small Negative Ion Facility at CCFE is continuing to improve in reliability, with great improvements made in the RF system. Understanding of the system has greatly increased, and will allow further improvements to be made, in particular to the shielding and earthing system.

Diagnostic systems have also developed well, with visible cameras, the instrumented beam target and spectrometer all ready for regular use. Data analysis is continuing to develop through modelling. A Langmuir probe system will be added shortly to allow further measurements in the extraction region. This will use the Boyd-Twiddy method [8] to directly measure the electron energy distribution function.

With increased diagnostic capability and good reliability, characterisation of the source in its current setup will be completed. This will be followed by investigations into alternative materials to caesium for negative ion enhancement, and also an investigation into RF coupling frequency by replacing the current 13.56MHz power supply with one operating at 2MHz.

ACKNOWLEDGMENTS

This project has received funding from the European Union's Horizon 2020 research and innovation programme under grant agreement number 633053 and from the RCUK Energy Programme [grant number EP/I501045]. The views and opinions expressed herein do not necessarily reflect those of the European Commission.

REFERENCES

1. J. Zacks, R. McAdams et al, [AIP Conference Proceedings](#) 1515, 569 (2013) , Third International Symposium on Negative Ions, Beams and Sources (NIBS 2012)
2. G. Cunge, B. Crowley, D. Vender, M. M. Turner, [Plasma Sources Sci. Technol.](#) **8**, 576 (1999).
3. Langmuir and Mott-Smith *Gen. Elect. Rev.* 27 ,449, 1924
4. P. McNeely, S. V. Dudin et al, [Plasma Sources Sci. Technol.](#) 18 (2009) 014011 (17pp)
5. E. Surrey, B. Crowley, [Plasma Phys. Control. Fusion](#) 45 (2003) 1209–1226
6. U. Fantz at al, [Nucl. Fusion](#) **46** (2006) S297–S306
7. I. Day, S. Gee, Proceedings of the 24th Symposium on Fusion Technology, Warsaw, Poland, 11th September 2006
8. R. L. F. Boyd and N. D. Twiddy, 1959 *Proc. R. Soc. A* **53** 250.